Correlation functions and statistical properties of xerogel (Sn, Ti, Zr)O_2

E. Z. Valiev, S. G. Bogdanov, A. N. Pirogov, L. M. Sharygin and V. I. Barybin

Institute of the Physics of Metals, Urals Department, Russian Academy of Sciences
(Submitted 25 May 1992; resubmitted 24 September 1992)
Zh. Eksp. Teor. Fiz. **103**, 204–212 (January 1993)

The spatial dependence of density-density correlation functions of a number of samples of xerogel (Sn, Ti, Zr)O_2 was determined from the experimental results obtained by a number of authors, using the method of the inverse Fourier transform. These results were used for the analysis of the level of density fluctuations in the xerogel and for the calculation of the correlation length. For a completely random porous structure, the size distribution function of the pores was obtained and a qualitative comparison was carried out with the experimental results by determining the dimensions of the pores from sorption isotherms of benzene vapor.

INTRODUCTION

This paper is devoted to the determination of the parameters of the porous structure (PS) of xerogels from data on small-angle neutron scattering (SANS).

Sorption methods are usually employed for the analysis of the PS of xerogels. However, they do not always permit us to obtain reliable quantitative information on the parameters of the PS.

In the present paper, we use the diffraction method for the investigation of the PS. This method was proposed in Refs. 1 and 2. In our opinion, only a thorough study of the random structure of xerogels by different methods can give us sufficient information on its properties. This information is necessary for understanding the sorption properties of xerogels and for forecasting new regions of their commercial application. In contrast to the sorption methods, diffraction method uses a method traditional in theoretical physics to describe the structure of the spatial disorder of objects that is

Plots of small-angle neutron scattering were given in Ref. 3 for 11 samples of xerogel (Sn, Ti, Zr)O_2 at different annealing temperatures T_{ann}. For the interpretation of these curves, we used the model of randomly distributed matter of uniform density.[1,2] Note that, according to this model, the neutron scattering cross section of a unit volume of a porous solid is

$$\frac{d\Sigma}{d\Omega} = 4\pi c(1-c)\rho_0^2 \int \gamma(r) r^2 \frac{\sin qr}{qr} dr. \qquad (1)$$

Here c is volume fraction of the solid phase, q is the modulus of the scattering vector, ρ_0 is the density of the neutron-scattering amplitude, $\gamma(r) = \langle \eta(0)\eta(r)\rangle / \langle \eta^2 \rangle$ is the pair correlation function of the random quantity $\eta = \rho - \rho_0 c$; $\langle \eta \rangle = 0$; $\langle \eta^2 \rangle = \rho_0^2 c(1-c)$.

Another but equivalent expression for $\gamma(r)$ is

$$\gamma(r) = \frac{Z(r) - c}{1-c}. \qquad (2)$$

$Z(r)$ is the probability that both ends of a rod of length r are in the solid phase.

In order to explain the observed curves of SANS, we assumed a simple form (in Ref. 3) for $\gamma(r)$:

$$\gamma(r) = \begin{cases} \gamma_1, & R_1 > r > 0, \\ -\gamma_2, & R_1 \leqslant r \leqslant R_2, \\ 0, & r > R_2, \end{cases} \qquad (3)$$

γ_1 and γ_2 are certain constants.

The calculated curves, obtained with the help of Eqs. (1) and (3), agree satisfactorily with the experimental curves in shape, and give, for certain R_1 and R_2, values for the scattering cross section that are close in absolute value to the observed values.[3]

However, the expression (3) is a very rough approximation and does not permit us to compare the correlation functions of the xerogels (Sn, Ti, Zr)O_2 with the correlation functions of other porous compounds.

SPATIAL DEPENDENCE OF THE CORRELATION FUNCTIONS OF XEROGEL (Sn, Ti, Zr)O_2

In the present paper, the correlation functions are determined with the help of the inverse Fourier transform of Eq. (1).

It follows from (1) that

$$\gamma(r) = [2\pi^2 \rho_0^2 c(1-c)]^{-1} \int_0^\infty q^2 \frac{d\Sigma}{d\Omega} \frac{\sin qr}{qr} dq. \qquad (4)$$

Substituting the experimental data for $d\Sigma/d\Omega$ in the integrand of (4), and carrying out the integration, we obtain the $\gamma(r)$ dependence. In carrying out the inverse Fourier transform in practice, a well known difficulty is that the experimentally measured quantity $d\Sigma/d\Omega$ is frequently unknown over the infinite interval of variation of q. In our case, we have succeeded in avoiding this difficulty since it follows form Ref. 3 that as $q \to \infty$, the quantity $d\Sigma/d\Omega \sim q^{-n}$ for all the samples investigated. The numerical values of the exponent n are given in Ref. 3. That is, in place of the absent experimental data we can use an analytic power dependence. The absence of experimental points for very small q is weakly shown in the final results because of the factor q^2 in the integrand of (4).

Figure 1a shows the function for the sample with annealing temperature of 500 °C obtained in such fashion. The result of the calculation is stable, i.e., smoothing and nonsmoothing of the experimental data for $d\Sigma/d\Omega$ lead to an insignificant difference in $\gamma(r)$. This also confirms the inverse calculation of the cross section from the given correlation functions. Figure 1b shows by a solid curve the curve $d\Sigma/d\Omega$, calculated according to Eq. (1) with the function $\gamma(r)$ from Fig. 1a. The correlation functions for the remain-

 1063-7761/93/010111-05$10.00 © 1993 American Institute of Physics

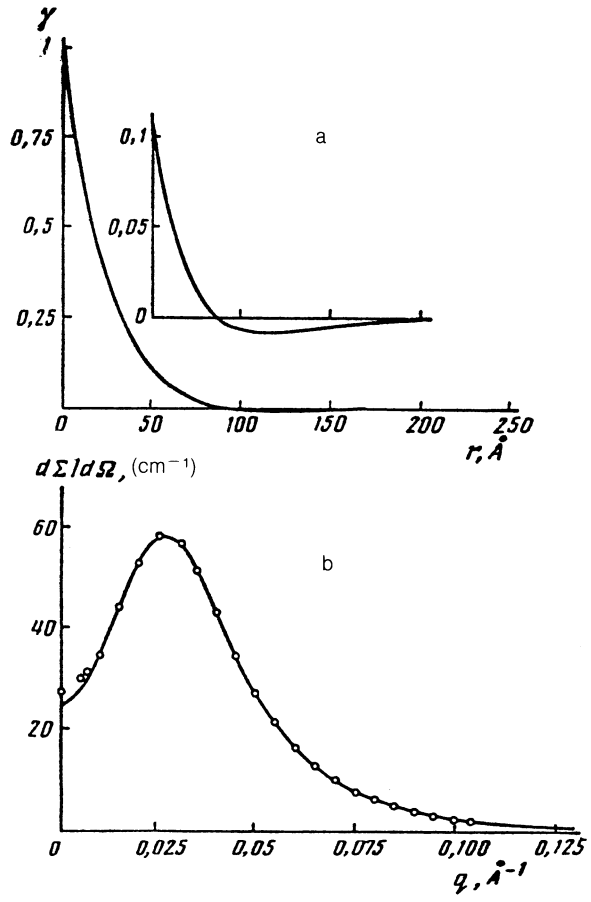

FIG. 1. a—Spatial dependence of the density-density correlation function for a sample with $T_{ann} = 500$ °C. Insert: portion of curve for $r > 50$ Å given in enlarged scale; horizontal scale, the same as in the main drawing. b—Differential neutron scattering cross section.—calculation from Eq. (1) with the function $\gamma(r)$ from Fig. 1a. 0—experimental points for a sample with $T_{ann} = 500$ °C.

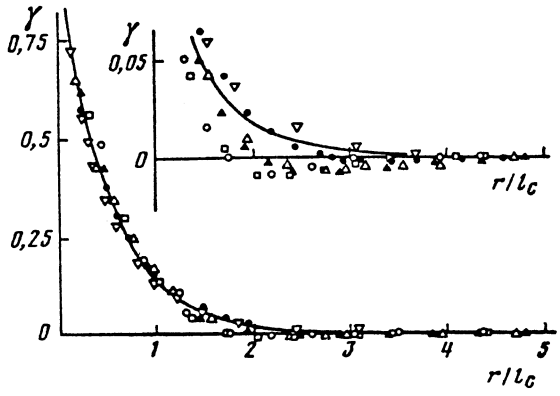

FIG. 2. Dependence of γ on r in reduced coordinates. —$\exp\{-2r/l_c\}$; ○)—for a sample with $T_{ann} = 200$ °C; □—300 °C; ▲—500 °C; △—700 °C; ●—800 °C:—▽–900 °C.

ing investigated samples were obtained in similar fashion.

Knowing the correlation function, we can calculate the correlation length $l_c = 2\int_0^\infty \gamma(r)dr$. The numerical values of the correlation lengths for samples with annealing temperatures 200 °C, 300 °C, 400 °C, 500 °C, 600 °C, 700 °C, 800 °C, and 900 °C, are equal to 22.9, 29.3, 33.8, 41.2, 44.0, 50.6, 81.7, and 162.4 Å.

Figure 2 shows the dependence of the correlation function on the reduced coordinate r/l_c for samples annealed at different temperatures. The function $\gamma(r) = \exp\{-r/a\}$, $l_c = 2a$ is indicated there by the solid curve. This describes the correlation density in the structure with completely random shape and distribution of pores.[1] The horizontal scale on inset of Fig. 2 is the same as in the in the rest of the drawing.

As is seen from Figs. 1a and 2, the correlation functions of the porous structure of the xerogel (Sn, Ti, Zr)O_2 are negative in the interval $2 \lesssim r/l_c \lesssim 3.5$, which agrees with the approximation (3) for $\gamma(r)$. It also follows from this that around each region filled with the solid phase, there exists a circle in which the density of the solid phase is less than the mean density of the material in the sample. The latter assertion can be understood if we use the definition (2) for $\gamma(r)$.

Formally, the region of negative values of $\gamma(r)$ is connected with the existence of a maximum in the scattering curve for $q \neq 0$. This fact leads us to the expression (3) for $\gamma(r)$ in the explanation of the experimental curves $d\Sigma/d\Omega$ in Ref. 3.

If we compare the xerogel with a binary substitutional alloy, then a porous structure with an exponential correlation function evidently corresponds to a completely disordered alloy, while the porous structure of the xerogel (Sn, Ti, Zr)O_2 recalls the structure of a binary alloy with short-range order. In the case of the xerogel, the short-range order in the organization of the solid phase and the cavity (pores) is connected with the presence of interaction between the particles of the solid phase at the early stages of formation of gel and drying of the gel-spheres. We recall that our samples were obtained by the sol-gel method.[4] In solid solutions, the short-range order is determined by the interaction between the atoms and the picture of scattering by neutrons is similar to ours. Compare the corresponding curves in Refs. 3 and 5.

It can be seen in Fig. 2 that the region of negative values of $\gamma(r)$ is more clearly expressed in samples with low annealing temperatures. With increase of the annealing temperature, information on the initial stage of formation of the structure "is forgotten" and the correlation functions become closer to exponentials, as is typical of completely random porous structures.

The data of Fig. 2 exhibit the known behavior of a porous structure for xerogel samples (Sn, Ti, Zr)O_2 with different annealing temperatures. An exception is the region of negative values of $\gamma(r)$, where the correlation functions of the samples with different annealing temperatures differ widely. In this entire region, however, the absolute values of $\gamma(r)$ are very small.

It is important to note the insignificant differences of the functions $\gamma(r)$ of all the investigated samples from the exponential dependence that is characteristic for a completely random porous structure which, as we are trying to show, achieves a rather complete analytic description.

DENSITY FLUCTUATIONS AND THE POROSITY OF THE XEROGEL

It is well known that the scattering intensity at small angles is determined by the fluctuations of the scattering amplitude.[2] In our case, the scattering cross section at zero

angle is connected with the density fluctuations of the solid phase in the sample by the following relation:

$$\frac{d\Sigma}{d\Omega}(0)=\langle\eta^2\rangle\int\gamma(r)dV=\int\langle\eta(0)\eta(r)\rangle\,dV. \qquad (5)$$

Under equilibrium conditions the level of the density fluctuations are determined by the isothermal compressibility $\beta = -(1/V)(\partial V/\partial P)_T$:

$$kT\beta=4\pi c(1-c)\int_0^\infty\gamma(r)r^2\,dr=\frac{d\Sigma}{d\Omega}(0)\rho_0^{-2}. \qquad (6)$$

The values of the bulk modulus $B^*=\beta^{-1}$, obtained from the experimental data by SANS with the use of Eq. (6) is shown in Fig. 3. The quantity P_m —strength of the xerogel, obtained by experiment on crushed granules, are shown in the same figure. If we assume that the bulk modulus of the granules of xerogel for static loading is $B\sim P_m$, then the large difference in the values of B and B^* should indicate the strong nonequilibrium of the structure of the xerogel. Thus the value of B^* characterizes not the equilibrium compressibility, but the level of density fluctuations in the sample. It follows from the numerical values of B^* that, the level of the density fluctuations of the xerogel is closer to that of a gas than to that of a solid.

The strength of the xerogel falls with increase in the annealing temperature and the density fluctuation level. This is seen from Fig. 3. Moreover, in our case, the evolution of the porous structure is accompanied by an increase in the density fluctuations.

Such a picture of the evolution of the porous structure is not always observed. For example, in Ref. 6 a case was noted in which the strength increased in the xerogels (Ti, Zr)O_2 upon increase in the annealing temperature. The increase in the strength was accompanied by a considerable decrease in the linear size of the granules, that is, a decrease in the porosity. The value of the density fluctuations should also decrease in such a case.

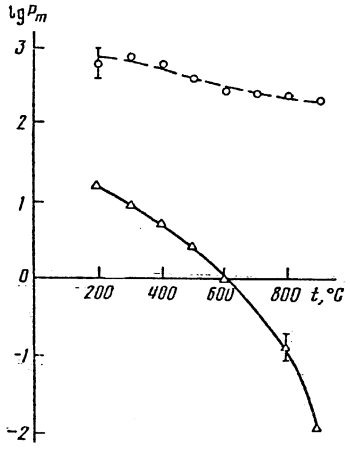

FIG. 3. Strength P_m and B^* as functions of the annealing temperature. The data are given in logarithmic coordinates. For $T_{ann}=200$ °C: $P_m\simeq 500$ kg/cm^2; $B^*\simeq 18$ kg/cm^2. ○—P_m, △—B^*.

In the xerogels (Sn, Ti, Zr)O_2, the size of the granules changes insignificantly in the annealing (by several percent), the disruption of the porous structure takes place at almost constant porosity and is accompanied by an increase in the density fluctuations. The correlation length increases from ~ 20 Å for a sample with $T_{ann}=200$ °C to ~ 160 Å for a sample with $T_{ann}=900$ °C. Thus, the mechanism of disruption of the porous structure in the annealing recalls the mechanism of disruption of long-range order in second-order phase transitions.

The difference in the evolution of the structure of the pores in our case and in Ref. 6 is evidently connected with the various diffusion processes, which play a decisive role in the sintering of the xerogels (Sn, Ti, Zr)O_2 and (Ti, Zr)O_2. In this connection, see, for example, Ref. 7, p. 211.

To conclude this section, we note that for a porous structure with correlation function $\gamma(r)=\exp\{-r/a\}$ the absolute value of the density fluctuations is 3–4 times that for the porous structure of xerogels with short-range order for the same correlation lengths. That is, the short-range order in the arrangement of the solid phase and of the pores in the xerogels decreases the density fluctuations, just as the short-range order in ordered alloys decreases the concentration fluctuations. The aforementioned decrease in the concentration fluctuations refers to the case in which we compare a completely disordered alloy and an alloy having the same composition but a short-range order.

PORE SIZE DISTRIBUTION

The correlation function of the xerogels (Sn, Ti, Zr)O_2 is close to exponential, which characterizes a completely random porous structure.[1] It is useful to compare the properties of the xerogels (Sn, Ti, Zr)O_2 with the properties of materials with a completely random structure.

In the case $\gamma(r)=\exp\{-r/a\}$, we have from Eq. (1),

$$\frac{d\Sigma}{d\Omega}=\frac{8\pi a^3\rho_0^2c(1-c)}{(1+q^2a^2)^2}. \qquad (7)$$

From Eqs. (9)–(11), we obtain (see Ref. 8, p. 29)

$$\frac{S}{V}=-4c(1-c)\gamma'(0)=\frac{4c(1-c)}{a}. \qquad (8)$$

It follows from (7) and (8) that the model of a solid phase of uniform density and fully distributed atmits of a simple analytic description containing the parameters a and c which are easily determined from experiment. Let us see how the pore-size distribution is obtained for this model.

Following Ref. 8, we consider a generalized-telegraph random process for the quantity

$$\eta(r)=z_{n(0,r)}, \qquad (9)$$

$n(0,r)$ is a random sequence of integers, such that the probability of n points landing on the interval (r_1, r_2) is

$$P_{n(r_1,r_2)}=\frac{[\overline{n(r_1,r_2)}]^n}{n!}\exp\{-\overline{n(r_1,r_2)}\},$$
$$\overline{n(r_1,r_2)}=a^{-1}|r_1-r_2|, \qquad (10)$$

$\overline{n(r_1,r_2)} = a^{-1}|r_1 - r_2|$; a^{-1} is the average number of points landing on a unit-length interval, z_i are statistically independent random quantities having a distribution

$$P(z)=c\delta(z-\rho_0(1-c))+(1-c)\delta(z+\rho_0 c). \qquad (11)$$

From (9)–(11) we obtain (see Ref. 8, p. 29)

$$\langle\eta(r)\rangle=0,\ \langle\eta^2\rangle=\rho_0^2 c(1-c),\ \langle\eta(0)\eta(r)\rangle=\langle\eta^2\rangle\exp\{-r/a\}.$$

Comparing these formulas and the expressions that follow Eq. (1), we see that the model of randomly distributed matter of uniform density, in the case $\gamma(r) = \exp\{-r/a\}$, has the same statistical properties as the random processes for the quantity from (9).

We compare the distribution of interval lengths between jumps of the quantity from (9) with the size distribution for matter and pores in the model of a randomly distributed solid phase. In the special case of $c = 1/2$ the pores and the matter have the same size distribution.

Then the probability density of the pore size distribution has the form (compare with Ref. 9, p. 26):

$$Y(r)=a^{-2}r\exp\{-r/a\}. \qquad (12)$$

The mean size of the pores from (12) is $\langle r\rangle = 2a$ and the variance is $\langle r^2\rangle - \langle r\rangle^2 = 2a^2$.

Since $c \simeq 1/2$ for our xerogels, the expression (12) can be compared with the experimental pore-size distribution curves determined from the sorption isotherms of benzene vapors.

Curve 2 in Fig. 4 represents the pore size distribution from the desorbed portion of the sorption isotherm for a sample with $T_{ann} = 200$ °C. Curve 3 represents the pore size distribution from the adsorption part of the sorption isotherm. Curve 1 is calculated from Eq. (12) for $a = 10$ Å. In spite of the fact that the mean pore sizes, determined from curves 1 and 2, are both approximately equal to 20 Å, the calculated curve 1 gives a broader pore-size distribution than the adsorption experiment, which can be due to the

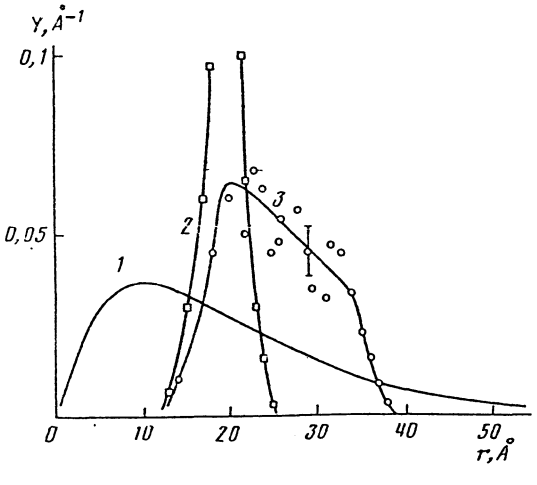

FIG. 4. Pore size distribution probability density. 1—calculated from formula in text; 2—experiment for sample with $T_{ann} = 200$ °C from the desorption portion of the soprtion isotherm of benzene vapor; 3—the sample from the adsorption portion of the sorption isotherm.

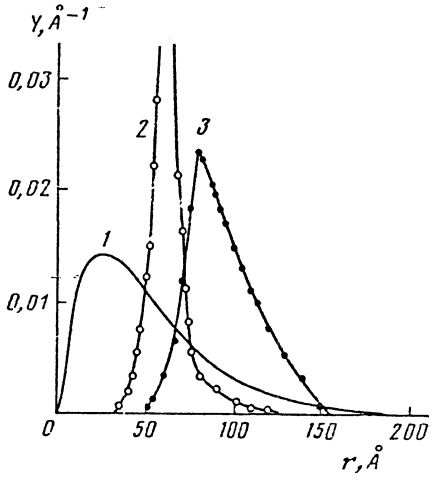

FIG. 5. Pore size distribution. 1—calculated from the formula in the text, $2a = 41$ Å; 2, 3—experiment for sample with $T_{ann} = 700$ °C from the adsorption and adsorption portions, respectively, of the sorption isotherm.

short-range order in the xerogel (Sn, Ti, Zr)O_2 which leads to a more homogeneous size of the pores than follows from the completely random porous structure. The pore distribution, determined from the adsorption isotherm, is broader than that from the desorption curve. This was to be expected, since the desorption branch of the isotherm is used to determine the throat radius of the pores for the globular dispersive body, while the adsorption branch determines the radius of curvature of the adsorption film.

The same can be said regarding a sample with $T_{ann} =$ 700 °C, the pore distribution curves for which are shown in Fig. 5.

It must be said that there exists another method for the determination of the pore size distribution function from the data of SAS.[10,11] The application of the method suggested in Refs. 10, 11 is made difficult in our case by the fact that for the xerogels (Sn, Ti, Zr)O_2 the interference effects in the scattering cross section are essential and these xerogesl cannot be regarded as dilute relative to the pores or solid phase.

CONCLUSION

From the results of Ref. 3 and the exposition above it follows that experiments on the scattering of neutrons allow us to obtain equally complete information on the porous structure as the adsorption methods (see Ref. 12). The comparison of the results that are determined by the above methods must promote both the reliable determination of the parameters of the porous structure and the progress in the development of these methods. The authors thank V. M. Galkin for help in the reduction of the experimental results.

[1]P. Debye, H. R. Anderson, and H. Brumberger, J. Appl. Phys. **28**, 679 (1957).
[2]A. Guinier and G. Fournet, *Small-Angle Scattering of X-Rays*, Wiley, New York-London, 1955, p. 46.
[3]É. Z. Valiev, S. G. Bogdanov, Yu. A. Dorofeev, A. N. Pirogov, L. M. Sharygin, V. I. Barybin, and O. Yu. Smyshlyaeva, Zh. Eksp. Teor. Fiz. **100**, 1000 (1991) [Sov. Phys. JETP **73**, 552 (1991)].
[4]L. M. Sharygin, V. F. Gonchar, and V. E. Moiseev, *Ion Exchange and*

Ionometry (in Russian) Leningrad State University, Leningrad USSR, 1986, Vol. 5, p. 9.
[5]Ya. S. Umanskii, *X-Radiography of Metals* (in Russian), Metallurgiya, Moscow, 1967, p. 117.
[6]L. M. Sharygin, T. G. Malykh, Yu. A. Dorofeev, and S. Ya. Tret'yakov, *Adsorption and Adsorbents*, Naukova Dumka, Kiev, 1983, v. 2, p. 44.
[7]Ya. I. Frenkel', *Introduction to the Theory of Metals*, Nauka, Leningrad, 1972.
[8]V. I. Klyapkin, *Stochastic Equations and Waves in Randomly Disordered Media*, Nauka, Moscow, 1960.
[9]W. Feller, *An Introduction to the Probability Theory and its Applications*, Wiley, New York, 1950, vol. 2.
[10]J. Mering and D. Tchoubar, J. Appl. Cryst. **1**, 153 (1968).
[11]A. F. Shurov, T. A. Ershhova, and V. P. Kalinin, Kristrallogr. **21**, 688 (1976) [Sov. Phys. Crystallography **21**, 390 (1976)].
[12]S. Greg and K. Sing, *Adsorption, Surface Area, and Porosity*, Academic Press, New York, 1967.

Translated by R. T. Beyer